

Porphyrin-functionalized oligo- and polythiophenes†

Michael Schäferling^a and Peter Bäuerle^{*b}

^aInstitute of Analytical Chemistry, Chemo- and Biosensors, University of Regensburg, 93040 Regensburg, Germany

^bDepartment of Organic Chemistry II (Organic Materials and Combinatorial Chemistry), University of Ulm, Albert-Einstein-Allee 11, 89081 Ulm, Germany

Received 21st October 2003, Accepted 9th January 2004

First published as an Advance Article on the web 19th February 2004

The synthesis and properties of a series of bi- and terthiophenes **3–8** substituted with *meso*-tetraphenylporphyrin (TPP) groups *via* an isolating oxaalkyl chain is described. Electrooxidative polymerization leads to the corresponding metal complexed porphyrin-functionalized polythiophenes **P4–P8**. The electrochemical and spectroscopic properties of the polymer films reveal the superimposition of the electronic properties of the individual π -systems. Spectroelectrochemical experiments and conductivity measurements point to a mixed charge transport mechanism. Polaronic and bipolaronic delocalization on the conjugated chains combined with electron hopping processes *via* the porphyrin redox centers result in high stability of the polymers against overoxidation. Importantly, hybrid materials have been obtained which at the same time exhibit properties of a conducting polymer and a redox polymer that can be used for the detection of polychlorinated phenols in amperometric sensors.

Introduction

Functionalization of conducting polymers with groups providing specific physical and chemical properties, in addition to the particular electronic properties of the conjugated backbone, has become more and more prominent in recent years.¹ These so-called “intelligent” materials are promising candidates for sensor,^{2,3a} electrochromic,⁴ redox catalytic⁵ or energy conversion applications.⁶ In this respect, polypyrroles or polythiophenes substituted with redox or molecular recognizing groups⁷ represent very attractive combinations. To this end, electrochemically reversible acceptor groups such as viologens,⁸ quinones⁹ or fullerenes,¹⁰ and correspondingly, donor groups like ferrocene,³ tetrathiafulvalene¹¹ or metal complexes^{9a,12} have been covalently linked to conducting backbones. The interplay between these functional groups and the conducting polymer backbone has been investigated.

Only a few examples are known of the combination of conjugated polymers and porphyrins which show multi-redox behaviour. Several attempts have been undertaken to prepare porphyrins bearing pyrrole, aniline or phenoxy groups.¹³ Electrochemical polymerization, however, typically resulted in structurally undefined films lacking conducting matrices.¹⁴ Their electrochemical behaviour rather points to charge transport *via* electron hopping between the porphyrin moieties and thus to redox conductivity. Nevertheless, these polymers exhibited electrocatalytic activity in, *e.g.*, the epoxidation of cyclooctene or the oxidation of 2,6-di-*tert*-butylphenol to the corresponding quinone.¹⁵ More recently copolymers consisting of phenylene-vinylene and TPP-functionalized phenylene-vinylene blocks were chemically synthesized for applications in organic light emitting diodes.¹⁶

The immobilization of negatively charged porphyrins as dopants and counter anions into the positively charged conducting polymer matrix represents another approach.¹⁷ Applications of these hybrid materials in photovoltaic or fuel cells,¹⁸ in electrocatalysis where they serve as model systems for redox

enzymes such as cytochrome P-450 or peroxidases,^{15,18b} or in amperometric (bio-)sensors for the *in-situ* detection of nitric oxide in blood¹⁹ have been described.

Based on first experiments,²⁰ we now present the synthesis and properties of novel bi- and terthiophenes **3–8** which are covalently linked to (metalated) tetraphenylporphyrins *via* an oxaalkyl spacer. Their electropolymerization leads to corresponding porphyrin-functionalized polythiophenes **P4–P8** which are characterized electrochemically, optically and by *in-situ* conductivity measurements. We will discuss the charge transport mechanism in these novel hybrid materials and show a first application in an amperometric sensor.

Experimental

Electrochemistry

Electrochemical measurements and polymerizations were performed with a computer-controlled EG&G PAR 273 potentiostat in a three-electrode single compartment cell equipped with platinum working electrodes of 0.785 mm² area, a platinum wire counter electrode and an Ag/AgCl reference electrode. Cyclic voltammetry was carried out in dichloromethane solution (HPLC grade, distilled over P₄O₁₀ under argon and filtered over aluminium oxide (activity Super I), containing 0.1 M of tetrabutylammonium hexafluorophosphate (TBAHFP). All potentials were internally referenced to the ferrocene-ferrocenium redox couple.

Spectroelectrochemistry

Spectroelectrograms were recorded with a Perkin-Elmer Lambda 19 spectrophotometer in conjunction with an EG&G PAR 363 potentiostat. All optical measurements were carried out in a thin layer electrochemical cell according to Salbeck,²¹ incorporating a polished platinum disk electrode ($\phi = 6$ mm) as working electrode, an Ag/AgCl wire as reference electrode and a platinum sheet as counter electrode in acetonitrile (HPLC grade, filtered over activated aluminium oxide), TBAHFP (0.1 M). Solutions were deaerated by argon bubbling prior to each experiment, which was run under a argon atmosphere. Spectra were recorded in a reflection mode

† Electronic supplementary information (ESI) available: ¹³C-NMR and IR spectroscopic data. See <http://www.rsc.org/suppdata/jm/b3/b313296j>

at the platinum working electrode with the aid of a Y-type optical fibre bundle.

Conductivity measurements

The *in-situ* conductivities were recorded with a bipotentiostat from Jaisle (model PG10). Comb-like interdigital arrays of platinum on a quartz substrate (gap 10 μm) served as working electrodes,²² a parallel arranged platinum sheet as the counter electrode, and an Ag/AgCl wire as reference electrode. After the polymer film was deposited onto the interdigital structure, a constant potential of $V_D = 5\text{--}10$ mV (drain voltage) was applied between the two channels of the array.

Spectroscopic data

¹H-NMR spectra were obtained with a Bruker AMX 500 instrument in CDCl₃ referenced to Me₄Si as internal standard. Coupling constants *J* are given in Hertz. Complexation of the porphyrins with cobalt, iron and manganese ions causes huge paramagnetic shifts for the porphyrin signals and broad peaks without resolution of the multiplet structures. FD mass spectra have been recorded with a Varian MAT 711, FAB-spectra with a Finnigan TSQ 7000, high-resolved dynamic FAB-spectra with a Finnigan MAT 95. Elemental analyses were performed with an Elementar Vario EL system. Due to incomplete combustion, for some metalated porphyrins elemental analyses with a generally accepted error margin of 0.3% per element sometimes could not be obtained. In these cases, alternative high resolution mass spectra were recorded. Melting points of porphyrins were typically above 300 °C and could not be detected. ¹³C-NMR and FT-IR data are available as ESI.†

Synthesis of monomers and polymers

Materials. 5-(4-Phenoxy)-10,15,20-tritolyldiporphyrin,²³ 3-(5-bromopentyl)-2,2'-bithiophene and 3'-(5-bromopentyl)-2,2':5',2''-terthiophene²⁴ were prepared following published procedures. All solvents were purified and dried by standard methods prior to use. The metal salts were used without further purification.

General procedure for the etherification of ω -bromoalkyloligothiophenes 2a,b with 5-(4-phenoxy)-10,15,20-tritolyldiporphyrin 1. In a round bottomed flask, 1.40 mmol of porphyrin **1** was dissolved in 30 ml DMF under argon atmosphere. Subsequently, a solution of 90 mg KOH in 6 ml methanol was added with a small amount of dibenzo-18-crown-6. The deprotonated phenolic porphyrin gave a green coloured solution. Then 1.40 mmol bithiophene **2a** or terthiophene **2b**, dissolved in 15 ml DMF, were added dropwise to the solution. The mixture was stirred for 15 hours at 80 °C. After the conversion was complete (DC-control), the solvent was removed and the crude product was washed with ethanol and purified twice by column chromatography (chloroform/silica gel).

3-[5-(4-Phenoxy)-10,15,20-tritolyldiporphyrin]pentyl-2,2'-bithiophene (TPP-2T) 3a. The synthesis was performed according the general procedure. Bithiophene **3a** was obtained as a violet coloured powder in 88% yield. ¹H-NMR (CDCl₃, ppm) $\delta = -2.75$ (s, 2H, N-H), 1.80–1.65 (m, 4H, H_c, H_d), 1.98–1.91 (m, 2H, H_b), 2.63 (s, 9H, *p*-CH₃), 2.86 (t, ³*J*_(e,d) = 7.43, 2H, H_e), 4.16 (t, ³*J*_(a,b) = 6.25, 2H, H_a), 6.98 (d, 1H, ³*J*_(4,5) = 5.25, H₄), 7.08 (dd, 1H, ³*J*_(4',5') = 4.98, ⁴*J*_(3',5') = 3.61, H_{4'}), 7.15 (dd, 1H, ³*J*_(3',4') = 3.61, ⁴*J*_(3',5') = 1.39, H_{3'}), 7.21 (d, 2H, ³*J*_(m,o) = 7.50, 2H, H_m-Ar_A), 7.23 (d, ³*J*_(5,4) = 5.25, 1H, H₅), 7.32 (dd, ³*J*_(5',4') = 5.00, ⁴*J*_(5',3') = 1.38, 1H, H_{5'}), 7.53 (d, ³*J*_(m,o) = 7.83, 6H, H_m-Ar_{B-D}), 8.09 (d, ³*J*_(o,m) = 8.03, 8H, H_o-Ar_{A-D}), 8.85 (d, ³*J*_(β_1,β_2) = 1.16, 8H, H β). MS (FD, 8 kV) [M⁺] 906.3; [M]_{calc} 907.20. Anal. Calc. for C₆₀H₅₀N₄OS₂: C 79.38, H 5.56, N 6.18 S 7.07. Found C 78.91, H 5.65, N 5.96, S 6.92%.

3-[5-(4-Phenoxy)-10,15,20-tritolyldiporphyrin]pentyl-2,2':5',2''-terthiophene (TPP-3T) 3b. The synthesis was performed according the general procedure. Terthiophene **3b** was obtained as a violet coloured powder in 73% yield. ¹H-NMR (CDCl₃, ppm) $\delta = -2.75$ (s, 2H, N-H), 1.86–1.70 (m, 4H, H_c, H_d), 2.03–1.96 (m, 2H, H_b), 2.69 (s, 9H, *p*-CH₃), 2.87 (t, ³*J*_(d,e) = 7.53, 2H, H_e), 4.21 (t, ³*J*_(a,b) = 6.31, 2H, H_a), 6.99 (dd, ³*J*_(4,3) = 3.69, ³*J*_(4,5) = 5.32, 1H, H₄), 7.08 (dd, ³*J*_(4',5') = 3.59, ³*J*_(4'',3'') = 5.09, 1H, H_{4''}), 7.11 (s, 1H, H_{4'}), 7.18 (dd, ³*J*_(3',4') = 3.59, ⁴*J*_(3',5') = 1.34, 1H, H_{3'}), 7.22 (dd, ³*J*_(5,4) = 5.28, 1H, H₅), 7.25 (d, 2H, ³*J*_(m,o) = 8.00, H_m-Ar_A), 7.33 (dd, ³*J*_(5',4') = 5.27, ⁴*J*_(5',3') = 1.34, 1H, H_{5'}), 7.54 (d, ³*J*_(m,o) = 8.00, 6H, H_m-Ar_{B-D}), 8.09 (d, ³*J*_(o,m) = 8.03, 8H, H_o-Ar_{A-D}), 8.85 (s, 8H, H β). MS (FD, 8 kV) [M⁺] 988.3; [M]_{calc} 989.34. Anal. Calc. for C₆₄H₅₂N₄OS₃: C 77.65, H 5.30, N 5.66. Found C 77.15, H 5.60, N 5.53%.

General procedure for metal insertion into oligothiophene-substituted porphyrins according to the Adler method²⁵. The oligothiophene-substituted porphyrin **3a,b** was dissolved in a minimum amount of refluxing DMF under argon atmosphere. Three equivalents of the corresponding divalent metal salt (chloride or acetate) were added. After 2 hours the conversion of the reaction was controlled by DC or detected by the loss of red fluorescence under a 360 nm UV lamp. If necessary, more equivalents of the metal salt had to be added and the reaction mixture was heated under reflux for additional 30 minutes. After cooling the reaction mixture in ice water, the crude product was precipitated by adding an equal volume of water, washed with water and air dried. The product was purified by two sequential column chromatographies (1. CHCl₃/Al₂O₃ activity III; 2. CH₂Cl₂/silica gel) and dried at 130 °C in vacuum over P₄O₁₀.

3-[5-(4-Phenoxy)-10,15,20-tritolyldiporphyrin]cobalt(II)-pentyl-2,2'-bithiophene (Co(II)-TPP-2T) 4a. Synthesis was performed according the general procedure with 300 mg (0.33 mmol) porphyrin-bithiophene **3a** in 30 ml DMF. Yield: 170 mg (52%) of **4a** as a purple-red powder. ¹H-NMR (CDCl₃, ppm) $\delta = 2.33$ (br, 4H, H_c, H_d), 2.76 (br, 2H, H_b), 3.29 (br, 2H, H_e), 4.13 (s, 9H, *p*-CH₃), 5.32 (br, 2H, H_a), 7.32 (br, 2H, H_{4'}, H₄), 7.40 (br, 1H, H_{3'}), 7.43 (br, 1H, H₅), 7.56 (br, 1H, H_{5'}), 9.26 (br, 2H, H_m-Ar_A), 9.66 (br, 8H, H β), 13.08 (br, 6H, H_m-Ar_{B-D}), 15.92 (br, 8H, H_o-Ar_{A-D}). MS (FD, 8 kV) [M⁺] 963.2; [M]_{calc} 964.14. Anal. Calc. for C₆₀H₄₈N₄OS₂Co: C 74.75, H 5.02, N 5.81 S 6.65. Found C 74.48, H 5.04, N 5.89, S 6.56%.

3-[5-(4-Phenoxy)-10,15,20-tritolyldiporphyrin]cobalt(II)-pentyl-2,2':5',2''-terthiophene (Co(II)-TPP-3T) 4b. Synthesis was performed according the general procedure with 600 mg (0.6 mmol) porphyrin-terthiophene **3b** in 60 ml DMF. Yield: 295 mg (47%) of **4b** as a purple-red powder. ¹H-NMR (CDCl₃, ppm) $\delta = 2.30$ (br, 4H, H_c, H_d), 2.68 (br, 2H, H_b), 3.21 (br, 2H, H_e), 4.09 (s, 9H, *p*-CH₃), 5.22 (br, 2H, H_a), 7.05 (br, 2H, H₄; H_{4'}), 7.21 (br, 2H, H_{4'}, H₃), 7.35 (br, 2, H₅, H_{3'}), 7.46 (br, 1H, H_{5'}), 9.27 (br, 2H, H_m-Ar_A), 9.66 (br, 8H, H β), 13.06 (br, 6H, H_m-Ar_{B-D}), 15.92 (br, 8H, H_o-Ar_{A-D}). MS (FD, 8 kV) [M⁺] 1045.2; [M]_{calc} 1046.26. Anal. Calc. for C₆₄H₅₀N₄OS₃Co: C 73.47, H 4.82, N 5.36 S 9.19. Found C 73.16, H 4.87, N 5.34 S 9.06%.

3-[5-(4-Phenoxy)-10,15,20-tritolyldiporphyrin]nickel(II)-pentyl-2,2'-bithiophene (Ni(II)-TPP-2T) 5a. Synthesis was performed according the general procedure with 300 mg (0.33 mmol) porphyrin-bithiophene **3a** in 30 ml DMF. Yield: 210 mg (67%) of **5a** as a red powder. ¹H-NMR (CDCl₃, ppm) $\delta = 1.80\text{--}1.65$ (m, 4H, H_c, H_d), 1.98–1.91 (m, 2H, H_b), 2.63 (s, 9H, *p*-CH₃), 2.86 (t, ³*J*_(e,d) = 7.43, 2H, H_e), 4.16 (t, ³*J*_(a,b) = 6.25, 2H, H_a), 6.98 (d, 1H, ³*J*_(4,5) = 5.04, H₄), 7.07 (dd, 1H, ³*J*_(4',5') = 5.04,

$^4J_{(3',5')} = 3.64$, H₄), 7.14 (br, 1H, H₃), 7.19 (br, 1H, H₅), 7.21 (br, 2H, 2H, H_{m-Ar_A}), 7.31 (dd, $^3J_{(5',4')} = 5.04$, $^4J_{(5',3')} = 1.12$, 1H, H₅), 7.46 (d, $^3J_{(m,o)} = 7.84$, 6H, H_{m-Ar_{B-D}}), 7.88 (d, $^3J_{(o,m)} = 7.83$, 8H, H_{o-Ar_{A-D}}), 8.75 (d, $^3J_{(\beta_1,\beta_2)} = 1.40$, 8H, H_β). MS (FD, 8 kV) [M⁺] 963.0; [M]_{calc} 963.89. Anal. Calc. for C₆₀H₄₈N₄OS₂Ni: C 74.76, H 5.02, N 5.81 S 6.65. Found C 73.95, H 5.13, N 5.80, S 6.48%.

3-[5-(4-Phenoxy)-10,15,20-tritolyldiporphyrinylnickel(II)]pentyl-2,2':5,2''-terthiophene (Ni(II)-TPP-3T) 5b. Synthesis was performed according the general procedure with 500 mg (0.5 mmol) porphyrin-terthiophene **3b** in 50 ml DMF. Yield: 390 mg (74%) of **5b** as a red powder. ¹H-NMR (CDCl₃, ppm) $\delta = 1.84$ – 1.65 (m, 4H, H_c, H_d), 2.00– 1.95 (m, 2H, H_b), 2.64 (s, 9H, *p*-CH₃), 2.86 (t, $^3J_{(d,e)} = 7.43$, 2H, H_e), 4.19 (t, $^3J_{(a,b)} = 6.30$, 2H, H_a), 6.99 (dd, $^3J_{(4,3)} = 3.92$, $^3J_{(4,5)} = 5.04$, 1H, H₄), 7.08 (s, 1H, H_{4'}), 7.09 (dd, $^3J_{(4'',5'')} = 3.36$, $^3J_{(4',3')} = 5.32$, 1H, H_{4''}), 7.16 (br, 1H, H₃), 7.18 (br, 1H, H_{3''}), 7.20 (br, 1H, H₅), 7.23 (br, 2H, H_{m-Ar_A}), 7.33 (dd, $^3J_{(5',4')} = 4.76$, $^4J_{(5',3')} = 1.20$, 1H, H₅), 7.47 (d, $^3J_{(m,o)} = 7.84$, 6H, H_{m-Ar_{B-D}}), 7.89 (d, $^3J_{(o,m)} = 7.55$, 8H, H_{o-Ar_{A-D}}), 8.75 (d, $^3J_{(\beta_1,\beta_2)} = 1.68$, 8H, H_β). MS (FD, 8 kV) [M⁺] 1045.2; [M]_{calc} 1046.01. Anal. Calc. for C₆₄H₅₀N₄OS₃Ni: C 73.48, H 4.82, N 5.36. Found C 73.07, H 4.92 N 5.29%.

3-[5-(4-Phenoxy)-10,15,20-tritolyldiporphyrinyliron(III) chloride]pentyl-2,2'-bithiophene (Fe(III)Cl-TPP-2T) 6a. Synthesis was performed according the general procedure with 600 mg (0.66 mmol) porphyrin-bithiophene **3a** in 50 ml DMF. After two chromatographic purification steps the product was dissolved in CHCl₃ and shaken with 1 M HCl to cleave the formed green coloured μ -oxo-dimers to the iron(III) chloro complex. Yield: 500 mg (76%) of **6a** as a brown powder. ¹H-NMR (CDCl₃, ppm) $\delta = 1.94$ (br, 2H, H_c), 2.22 (br, 2H, H_d), 2.71 (br, 2H, H_b), 2.95 (br, 2H, H_e), 5.00 (br, 2H, H_a), 6.39 (s, 9H, *p*-CH₃), 6.96 (br, 1H, H₃), 7.06 (br, 1H, H_{4'}), 7.28 (br, 1H, H₄), 7.56 (br, 2H, H₅, H_{5''}), 11.36 (br, 2H, H_{o-Ar_A}), 12.00 (br, 6H, H_{o-Ar_{B-D}}), 12.60 (br, 2H, H_{m-Ar_A}), 13.27 (br, 6H, H_{m-Ar_{B-D}}), 78.40 (br, 8H, H_β). Dynamic high-resolution MS (+FAB) [M⁺] 960.2613; [M]_{calc} 960.2619.

3-[5-(4-Phenoxy)-10,15,20-tritolyldiporphyrinyliron(III) chloride]pentyl-2,2':5,2''-terthiophene (Fe(III)Cl-TPP-3T) 6b. Synthesis was performed according the general procedure with 230 mg (0.23 mmol) porphyrin-terthiophene **3b** in 25 ml DMF. After two chromatographic purification steps the product was dissolved in CHCl₃ and shaken with 1 M HCl to cleave the formed green coloured μ -oxo-dimers to the iron(III) chloro complex. Yield: 80 mg (32%) of **6b** as a brown powder. ¹H-NMR (CDCl₃, ppm) $\delta = 2.20$ (br, 4H, H_d, H_c), 2.49 (br, 2H, H_b), 3.17 (br, 2H, H_e), 5.31 (br, 2H, H_a), 6.40 (s, 9H, *p*-CH₃), 7.05 (br, 7H, H_{5''}, H₅, H_{4''}, H₄, H_{3''}, H₃), 11.51 (br, 2H, H_{o-Ar_A}); 7.50; 7.39; 7.35; 7.26; 7.22; 7.19; 12.05 (br, 6H, H_{o-Ar_{B-D}}), 12.57 (br, 2H, H_{m-Ar_A}), 13.21 (br, 6H, H_{m-Ar_{B-D}}), 76.70 (br, 8H, H_β). MS (FD, 8 kV) [M⁺] 1077.2; [M]_{calc} 1078.62.

3-[5-(4-Phenoxy)-10,15,20-tritolyldiporphyrinylmanganese(III) chloride]pentyl-2,2'-bithiophene (Mn(III)Cl-TPP-2T) 7a. Metal insertion was achieved by a variation of the procedure reported by Jones *et al.*²⁶ To 500 mg (0.57 mmol) porphyrin-bithiophene **3a**, dissolved in 50 ml refluxing DMF, 500 mg of Mn(III) acetate tetrahydrate were added. After complete conversion, the reaction mixture was poured in a solution of 15 mg sodium chloride in 50 ml ice water. The green precipitate was filtered, washed with 200 ml water and redissolved in 100 ml methanol. The solution was filtered again and poured into a 6 M hydrochloric acid solution. The green precipitate was collected by filtration, washed with water

and finally purified by column chromatography (CH₂Cl₂/Al₂O₃ activity III). The yield was 370 mg (65%) of a green powder. ¹H-NMR (CDCl₃, ppm) $\delta = -21.78$ (br, w, 8H, H_β), 1.67 (br, 2H, H_c), 1.80 (br, 2H, H_d), 1.96 (br, 2H, H_b), 2.86 (br, 2H, H_e), 3.00 (s, 9H, *p*-CH₃), 4.22 (br, 2H, H_a), 7.00 (br, 1H, H₃), 7.08 (br, 2H, H₄, H_{4'}), 7.14 (br, 8H, H_{m-Ar_{A-D}}), 7.30 (br, 2H, H₅; H₅), 8.11 (br, 8H, H-2, H_{o-Ar_{A-D}}). MS (+FAB/6–8 keV) [M⁺] 959.3; [M]_{calc} 960.13 for C₆₀H₄₈N₄OS₂Mn⁺. Anal. Calc. for C₆₀H₄₈N₄OS₂MnCl (*M_r* = 995.58): C 72.38, H 4.86, N 5.63. Found C 71.48, H 4.85 N 5.50%.

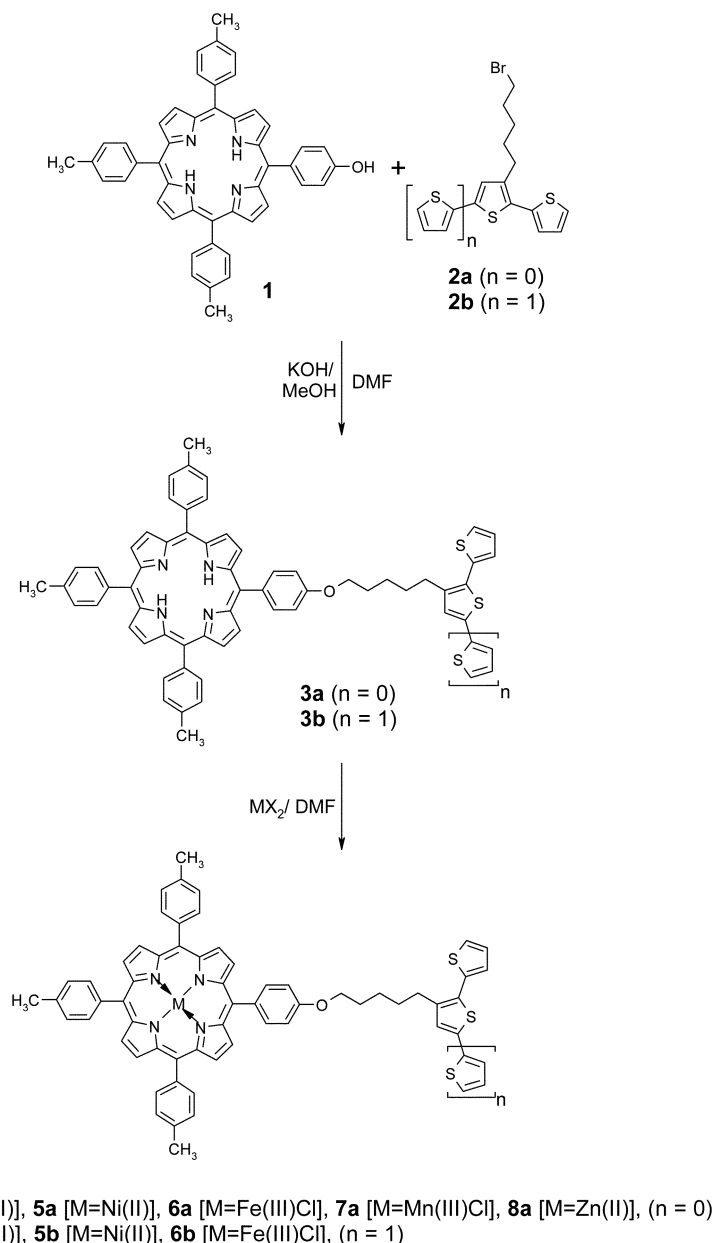
3-[5-(4-Phenoxy)-10,15,20-tritolyldiporphyrinylzinc(II)]pentyl-2,2'-bithiophene (Zn(II)-TPP-2T) 8a. Synthesis was performed according the general procedure with 550 mg (0.6 mmol) porphyrin-bithiophene **3a** in 50 ml DMF. Yield: 430 mg (73%) of **8a** as a purple powder. ¹H-NMR (CDCl₃, ppm) $\delta = 1.82$ – 1.67 (m, 4H, H_d, H_c), 1.97 (t, $^3J_{(b,c)(b,a)} = 7.14$, 2H, H_b), 2.70 (s, 9H, *p*-CH₃), 2.86 (t, $^3J_{(e,d)} = 7.28$, 2H, H_e), 4.19 (t, $^3J_{(a,b)} = 6.44$, 2H, H_a), 6.98 (d, $^3J_{(4,5)} = 5.32$, 1H, H₄), 7.07 (dd, $^3J_{(4',5')} = 5.04$, $^3J_{(4',3')} = 3.64$, 1H, H_{4'}), 7.14 (dd, $^3J_{(3',4')} = 3.36$, $^4J_{(3',5')} = 1.12$, 1H, H₃), 7.17 (br, 1H, H₅), 7.20 (d, $^3J_{(m,o)} = 1.40$, 2H, H_{m-Ar_A}), 7.31 (dd, $^3J_{(5',4')} = 5.04$, $^4J_{(5',3')} = 1.12$, 1H, H₅), 7.54 (d, $^3J_{(m,o)} = 7.84$, 6H, H_{m-Ar_{B-D}}), 8.09 (d, $^3J_{(o,m)} = 8.12$, 8H, H_{o-Ar_{A-D}}), 8.95 (d, $^3J_{(\beta_1,\beta_2)} = 0.54$, 8H, H_β). MS (FD, 8 kV) [M⁺] 969.3; [M]_{calc} 970.60. Anal. Calc. for C₆₀H₄₈N₄OS₂Zn: C 74.25, H 4.98, N 5.77. Found C 74.11, H 4.93, N 5.59%.

Results and discussion

Synthesis of porphyrin-functionalized oligothiophenes

The synthesis of the asymmetrically substituted porphyrin derivative 5-(4-hydroxyphenyl)-10,15,20-tritolyldiporphyrin (TPP) **1** was accomplished according to a variation of the Adler synthesis by reacting *p*-methylbenzaldehyde, *p*-hydroxybenzaldehyde and pyrrole in propionic acid.²⁵ Porphyrin **1** was obtained in 5.7% yield after chromatographic purification. The bithiophene and terthiophene building blocks **2a** and **2b**, respectively, bearing a 5-bromopentyl side chain were effectively synthesized according to protocols recently developed in our laboratory.²⁴ NBS-bromination of 3-(5-bromopentyl)thiophene in DMF yielded 2-bromo-3-(5-bromopentyl)thiophene in 66% yield which successively was cross-coupled with 2-thienylmagnesium bromide to provide 3-(5-bromopentyl)-2,2'-bithiophene **2a** in 29% yield. By analogous reaction, 2,5-dibromo-3-(5-bromopentyl)thiophene, which was obtained in 65% yield by dibromination of 3-(5-bromopentyl)thiophene with excess NBS, was converted with two equivalents of 2-thienylmagnesium bromide to yield the corresponding trimer, 3'-(5-bromopentyl)-2,2':5,2''-terthiophene **2b**, in 70% yield. The coupling of the porphyrin subunit to the oligothiophenes was carried out by a Williamson ether synthesis to give TPP-functionalised bithiophene (TPP-2T) **3a** (*n* = 0) in 88% yield and the analogous terthiophene (TPP-3T) **3b** (*n* = 1) in 73% yield (Scheme 1).

The insertion of metal ions into the porphyrin units was achieved by reacting TPP-functionalized oligothiophenes **3a,b** with divalent metal chlorides or acetates in refluxing DMF according to the method of Adler *et al.*²⁵ The corresponding divalent cobalt complexes **4a,b**, nickel complexes **5a,b** and zinc complex **8a** were obtained in good yields. For the preparation of the trivalent iron complexes **6a,b** and manganese complex **7a** we have used alternative methods (Scheme 1, Table 1).²⁶ In the case of the Fe(III)-complexes **6a,b**, metal-oxo-bridged dimers which are formed during the reaction were easily converted to the monomeric species by treatment of the dimers with HCl. The geometry and electronic configuration at the metal center have a strong influence on the ¹H- and ¹³C-NMR spectra of the various metal porphyrins. Particularly in the case of the



Scheme 1

high-spin Fe(III)Cl and Mn(III)Cl complexes **6** and **7**, signals due to the porphyrin subunit exhibit increased shifts with increasing number of unpaired electrons. However, the resonances of the oligothiophene moieties are less affected, because the influence of the paramagnetic central cation decreases with increasing distance. The shifts we find are in excellent accordance with values reported for TPP metal complexes.²⁷

Optical properties of the TPP-functionalized oligothiophenes

Optical absorption spectra of the novel porphyrin-oligothiophenes in dichloromethane exhibit typical bands of the individual subunits. In particular, these consist of an intense Soret-band

at around 420 nm, four weaker Q-bands between 510 and 650 nm due to the porphyrin moiety²⁸ and the π - π^* transition of the oligothiophene at 290 to 350 nm. Therefore, the pentyloxy spacer decouples the two chromophores electronically (Fig. 1). The intensity of the Soret-band decreases for the divalent Co, Ni and Zn complexes and is shifted to higher energies for Co(II) and Ni(II) and to lower energies for Zn(II). With respect to the parent compounds **3a,b** the number of Q-bands is decreased to two for Zn(II) and to one for Co(II) and Ni(II) (Fig. 2). Spectra of the Fe(III) and Mn(III) complexes additionally show an intense absorption at 350 to 400 nm which can be attributed to a charge transfer of the occupied π -orbitals of the porphyrin into vacant d-orbitals of the central

Table 1 Yields of the metal complexation of the TPP-functionalized oligothiophenes **3a,b**

Metal salt MX ₂	TPP-2T 3a	TPP-3T 3b
CoCl ₂ ·6H ₂ O	Co(II)-TPP-2T 4a (52%)	Co(II)-TPP-3T 4b (47%)
Ni(CH ₃ COO) ₂ ·4H ₂ O	Ni(II)-TPP-2T 5a (67%)	Ni(II)-TPP-3T 5b (74%)
FeCl ₂ ·4H ₂ O	Fe(III)Cl-TPP-2T 6a (76%)	Fe(III)Cl-TPP-3T 6b (32%)
Mn(CH ₃ COO) ₂ ·4H ₂ O	Mn(III)Cl-TPP-2T 7a (65%)	—
Zn(CH ₃ COO) ₂ ·2H ₂ O	Zn(II)-TPP-2T 8a (73%)	—

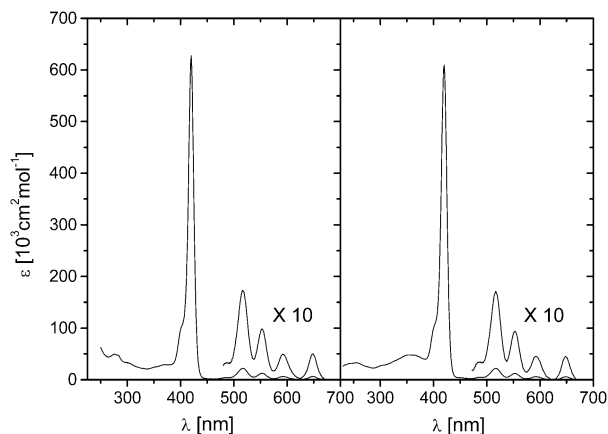


Fig. 1 Absorption spectra of TPP-functionalized bithiophene **3a** (left) and terthiophene **3b** (right).

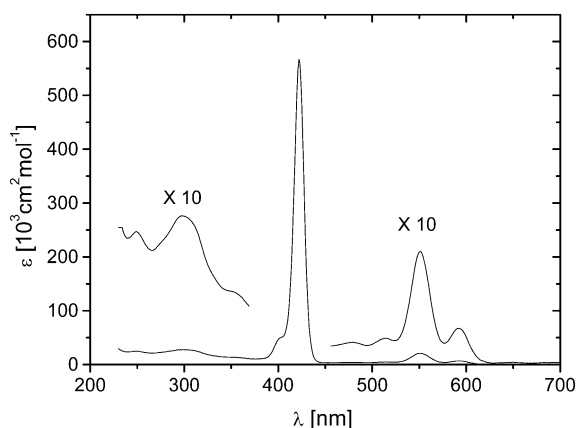


Fig. 2 Absorption spectrum of Zn(II)TPP-2T **8a**.

metal cation (Fig. 3).²⁸ In these cases, the maxima of the oligothiophene transitions were determined from difference spectra. The optical data are summarized in Table 2 and are in good accordance with data reported for metalated tetraphenylporphyrins.^{28,29}

Redox properties of the TPP-functionalized oligothiophenes

Cyclic voltammetry (CV) of the (metallo-)porphyrin-functionalized oligothiophenes **3–8** reveals the redox transitions of the individual subunits indicating their electronic decoupling in accordance with the optical data. The characteristic reversible multi-step redox chemistry of the porphyrin ligand includes several successive one-electron transitions (I,II reduction and III–V oxidation processes).³⁰ Additionally, the reversible redox waves of the central metal cation ($M^{n+(n+1)+}$) were detectable

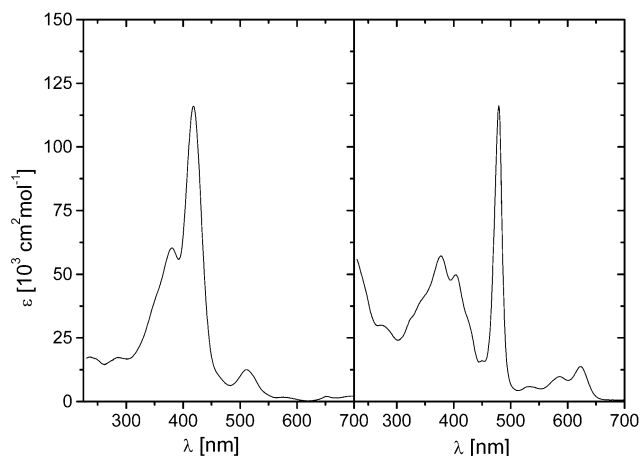


Fig. 3 Absorption spectra of Fe(III)Cl-TPP-2T **6a** (left) and Mn(III)Cl-TPP-2T **7a** (right).

for Co ($E^\circ = -1.44$ V, $E^\circ = 0.34$ V), Fe ($E^\circ = -0.84$ V) and Mn ($E^\circ = -0.81$ V). Furthermore, the typical irreversible oxidation of the bithiophene ($E_{pa} = 0.78–0.96$ V) and terthiophene units ($E_{pa} = 0.62$ V) in the positive potential regime could be determined only in some cases, because they are partially superimposed by the first or second oxidation wave of the porphyrin subunit. The redox data are summarized in Table 3. The examples of the metal-free porphyrin-oligothiophenes **3a,b** and the corresponding Fe(III)Cl complexes **6a,b** are illustrated in Fig. 4.

With respect to the parent compounds **3a,b**, the influence of the metal cations on the redox potentials of the porphyrin ring system is evident. Whereas Zn(II) increases the electron density in the π -system and shifts the oxidation waves to more negative potentials, electron withdrawing Ni(II), Co(II), Fe(III) and Mn(III) ions in this order give rise to a gradually increasing positive shift.³¹

Electropolymerization of the metalated TPP-functionalized oligothiophenes and characterization of the corresponding polythiophenes

Polymerization of the metal-free porphyrin-oligothiophenes **3a,b** by electrochemical oxidation of the oligothiophene subunit was not possible due to the interference of the porphyrin nitrogens with the oligothiophene radical cations. Consequently, oxidative electropolymerization of the metalated porphyrin-oligothiophenes **4–8** was successful either by potentiodynamic or by pulsed techniques at concentrations of 10^{-3} mol l⁻¹. Typically, positive turnover potentials of 0.9–1.0 V for the bithiophenes and of 0.7–0.8 V for the terthiophenes, respectively, were chosen. The growth of the conducting polymer is reflected by gradually increasing

Table 2 Absorption maxima and molar extinction coefficients of TPP-functionalized oligothiophenes **3a,b** and the corresponding metal complexes **4–8**

Compound	Oligothioph. $\pi-\pi^*$	Metal d-type	Soret		Porphyrin Q-bands		
	λ_{max}/nm (log ϵ)	λ_{max}/nm (log ϵ)	λ_{max}/nm (log ϵ)	λ_{max}/nm (log ϵ)	λ_{max}/nm (log ϵ)	λ_{max}/nm (log ϵ)	λ_{max}/nm (log ϵ)
TPP-2T 3a	290 (3.90)	—	420 (5.80)	517 (4.24)	553 (4.00)	592 (3.72)	648 (3.74)
TPP-3T 3b	344 (4.46)	—	420 (5.80)	517 (4.24)	553 (4.00)	592 (3.72)	648 (3.74)
Co(II)-TPP-2T 4a	304 (3.85)	—	412 (5.52)	529 (4.24)	—	—	—
Co(II)-TPP-3T 4b	346 (4.30)	—	412 (5.52)	529 (4.23)	—	—	—
Ni(II)-TPP-2T 5a	295 (4.00)	—	416 (5.46)	529 (4.29)	—	—	—
Ni(II)-TPP-3T 5b	345 (4.36)	—	416 (5.64)	529 (4.29)	—	—	—
[Fe(III)-TPP-2T]Cl 6a	293 (4.15)	381 (4.79)	511 (4.14)	511 (4.14)	577 (3.53)	—	—
[Fe(III)-TPP-3T]Cl 6b	341 (4.26)	378 (4.82)	512 (4.13)	512 (4.13)	576 (3.49)	—	—
[Mn(III)-TPP-2T]Cl 7a	290 (3.95)	378, 405 (4.76), (4.70)	480 (5.06)	480 (5.06)	531 (3.77)	587 (3.98)	623 (4.13)
Zn(II)-TPP-2T 8a	305 (3.70)	—	422 (5.75)	—	551 (4.30)	592 (3.79)	—

Table 3 Redox potentials of TPP-functionalized oligothiophenes **3a,b** and the corresponding metal complexes **4–8** (all potentials vs. Fc/Fc⁺)

Compound	Metalloporphyrin reduction		Metal cation		Metalloporphyrin oxidation			2T, 3T $E_{pa}(T)/V$
	$E(I)^a/V$	$E^\circ(II)/V$	$E^\circ(M^{1+/2+})/V$	$E^\circ(M^{2+/3+})/V$	$E^\circ(III)/V$	$E^\circ(IV)/V$	$E^\circ(V)/V$	
TPP-2T 3a	-2.03	-1.71	—	—	0.44	0.85	1.10	^b
TPP-3T 3b	-2.05	-1.70	—	—	0.46	0.87	1.10	0.62
Co(II)-TPP-2T 4a	-1.95	—	-1.44	0.34	0.51	0.75	1.34	^b
Co(II)-TPP-3T 4b	-1.95	—	-1.41	0.34	0.51	0.78	1.36	^c
Ni(II)-TPP-2T 5a	—	-1.81	—	—	0.50	0.84	1.29	^b
Ni(II)-TPP-3T 5b	—	-1.80	—	—	0.50	0.86	1.29	^c
[Fe(III)-TPP-2T]Cl 6a	—	-1.60	—	-0.86	0.55	0.98	1.24	0.87
[Fe(III)-TPP-3T]Cl 6b	—	-1.57	—	-0.84	0.55	0.99	1.26	^c
[Mn(III)-TPP-2T]Cl 7a	-2.14	—	—	-0.81	0.63	1.06	1.28	0.90
Zn(II)-TPP-2T 8a	—	-1.92	—	—	0.23	0.50	0.76 ^d	0.96

^a Electrochemically reversible transition E° for metal-free TPPs **3**, irreversible transition E_{pc} for Co and Mn complexes **4** and **7**. ^b Superimposed by redox wave IV of the porphyrin unit. ^c Superimposed by redox wave III of the porphyrin unit. ^d An additional reversible oxidation wave of the porphyrin appears at 1.31 V.

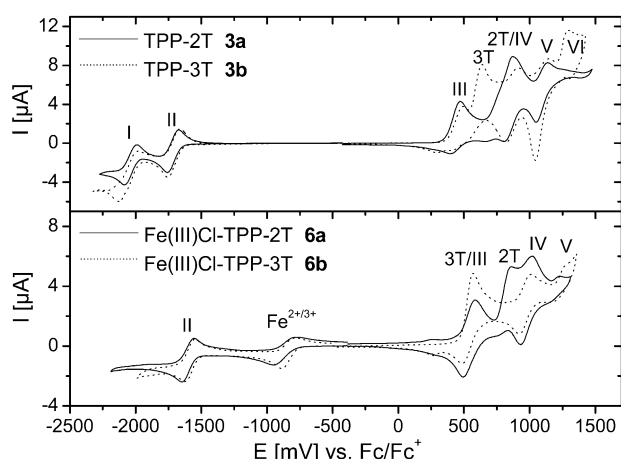


Fig. 4 Cyclic voltammetry of TPP-2T **3a** and TPP-3T **3b** (top); Fe(III)Cl-TPP-2T **6a** and Fe(III)Cl-TPP-3T **6b** (bottom) in CH₂Cl₂/TBAHFP (0.1 M), $c = 2 \times 10^{-3}$ mol l⁻¹, 100 mV s⁻¹.

currents in subsequent potential cycles and the simultaneous appearance of a new broad redox wave at potentials around 0.25 V which corresponds to the formation of the polythiophene backbone. We observed that porphyrin-functionalized bithiophenes **4a–8a** typically show a higher polymerization tendency and lead to thicker polymer films as compared to the corresponding terthiophenes. Under these optimized conditions the most stable polymer films resulted after 20–30 consecutive scans. These films show uniform properties, high reproducibility and good adhesion to the working electrodes. Solely, Mn(III)Cl-TPP-2T **7a** shows a low polymerization tendency and could only be electropolymerised by means of a pulse technique which also works for the polymerization of the other metalated porphyrin-oligothiophenes. Under variation of the conditions, the preparation of each polymer was optimized and reproduced several times.

The porphyrin-functionalized polythiophenes **P4–8** were electrochemically characterized in an electrolyte free of monomer. The CVs were taken at different scan speeds and in all cases clearly exhibit the combination of the typical symmetric and reversible redox waves of the conducting polythiophene backbone and the porphyrin redox centers. In recent studies, such a result could not be obtained by copolymers of 2,2'-bithiophene and a porphyrin-functionalized monothiophene.³² Charging of the polythiophene backbone starts at around 0 to 0.1 V and, typical for conducting polymers, results in a broad wave peaking at potentials around 0.15 to 0.2 V. At more positive potentials, the redox waves of the appended porphyrin units are superimposed and their redox potentials coincide well with those of the corresponding monomer unit.

Their peak separation is as expected small ($\Delta E = 10\text{--}40$ mV) and slightly deviates from the theoretical value of zero due to some flexibility given by the linear oxyalkyl spacer. The maximal currents linearly depend on the scan speed. Both facts clearly indicate the immobilisation of the porphyrin units on the electrode surface. The redox transitions of the central metal ions for the most part are hidden by the broad wave of the conducting backbone and could only be estimated. At negative potentials the CVs of the modified electrodes do not exhibit any charging and consequently electron transfer processes such as the reduction of the metal centres or of the porphyrin units do not occur. This is due to the rather insulating or at best semiconducting character of the polythiophene backbone in this potential regime. The polymer films show a very dense macroscopic structure and a quite compact morphology. Thus, a direct charge transfer from the electrode surface to the porphyrin units is rather unlikely. The cycling stability of the hybrid films is excellent for the poly(bithiophenes) **P4a–8a** and virtually no loss of the electroactivity after 100 cycles up to a reverse potential of 0.7 V can be seen. However, by reversing at a more positive potential (1.0 V) the electroactivity is reduced to about 85%. Overoxidation and irreversible chemical destruction of the polymer backbone visibly starts at around 1.1 V. This is in contrast to poly(alkylthiophenes) or poly(alkylbithiophenes) which are usually overoxidized at quite lower potentials. A poly(3-methyl-2,2'-bithiophene), which was prepared and characterized as a reference polymer under the same conditions, gave a similar film thickness and redox potential of the conjugated π -system. However, it was overoxidized at potentials of 0.6 to 0.7 V, values that correspond to literature data^{33a} and are 400 to 500 mV lower than those of the porphyrin-functionalized analogues **P4a–P8a**. We conclude from this finding that the high stability of our functionalized polythiophenes is due to partial charge transfer from the conducting backbone to the porphyrin moieties. Although, it should be noted that in other electrolytes poly(alkylthiophenes) have similar oxidation stabilities to those of our films.^{33b} The electrochemical data of the novel porphyrin-functionalized polythiophenes **P4–8** are collected in Table 4.

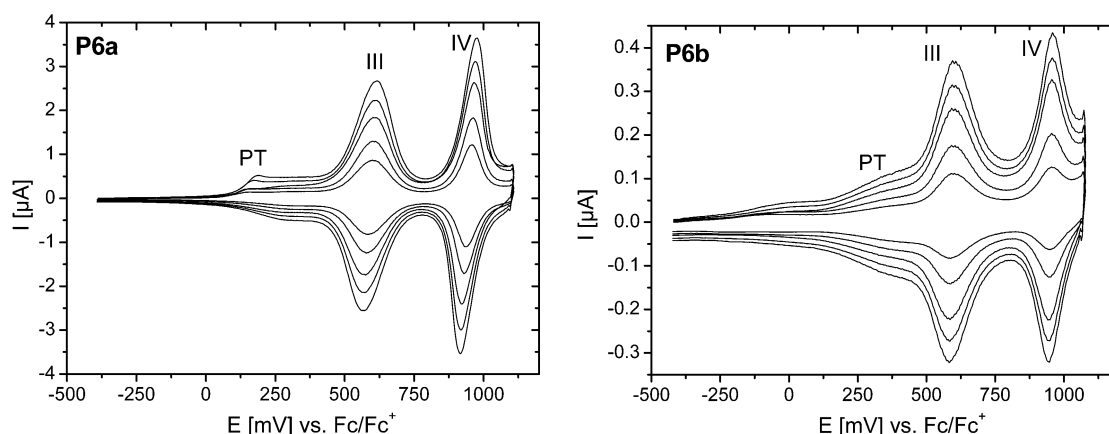
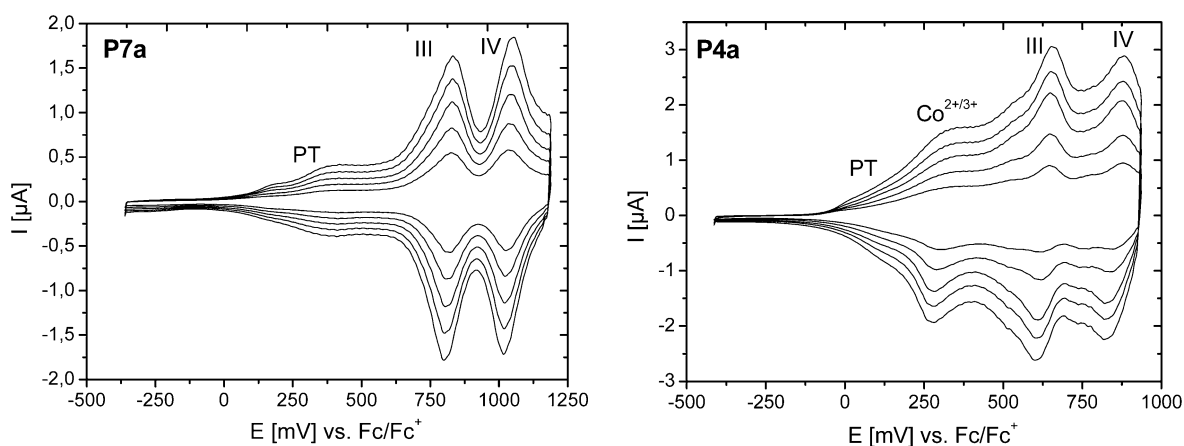
As typical examples, CVs of P[Fe(III)-TPP-2T] **P6a** in comparison to P[Fe(III)-TPP-3T] **P6b** and P[Mn(III)Cl-TPP-2T] **P7a** in comparison to P[Co(II)-TPP-2T] **P4a** are shown in Fig. 5 and 6, respectively. In conclusion, the electrochemical responses of the porphyrin-functionalized polythiophenes **P4–8** clearly indicate that they behave as a hybrid system consisting of a conducting polymer backbone and a redox polymer. The appearance of redox conductivity is assumed to be one reason for the observed increased stability of the polymers towards overoxidation.

We could further support this interpretation by *in-situ* conductivity measurements on a film of P[Co(II)-TPP-2T] **P4a**

Table 4 Redox potentials of metalloporphyrin-functionalized polythiophenes **P4–P8** (all potentials vs. Fc/Fc⁺)

Compound	Metal cation $E^\circ(\text{M}^{2+/3+})/\text{V}$	$E^\circ(\text{III})/\text{V}$ ($\Delta E/\text{mV}$) ^a	Metalloporphyrin $E^\circ(\text{IV})$ [V](ΔE [mV]) ^a	$E^\circ(\text{V})/\text{V}$ ($\Delta E/\text{mV}$) ^a	PT E_{pa}/V
P[Co(II)-TPP-2T] P4a	0.33	0.61 (40)	0.83 (40)	—	^b
P[Co(II)-TPP-3T] P4b	^c	0.59 (95)	0.77 (55)	—	0.20 ^b
P[Ni(II)-TPP-2T] P5a	—	0.56 (30)	0.79 (50)	—	0.15
P[Ni(II)-TPP-3T] P5b	—	0.55 (85)	0.79 (110)	—	0.16
P[Fe(III)Cl-TPP-2T] P6a	—	0.59 (30)	0.95 (55)	—	0.19
P[Fe(III)Cl-TPP-3T] P6b	—	0.59 (10)	0.95 (10)	—	^d
P[Mn(III)Cl-TPP-2T] P7a	—	0.82 (30)	1.04 (45)	—	0.19
P[Zn(II)-TPP-2T] P8a	—	0.30	0.62 (90)	0.84 (80)	0.18

^a Peak separation. ^b Superimposed by Co^{2+/3+}. ^c Superimposed by oxidation of the PT backbone. ^d Not resolved.

**Fig. 5** Cyclic voltammetry of P[Fe(III)Cl-TPP-2T] **P6a** and P[Fe(III)Cl-TPP-3T] **P6b** in CH₂Cl₂/TBAHFP (0.1 M), scan speeds 50, 75, 100, 125, 150 mV s⁻¹ from inwards to outwards.**Fig. 6** Cyclic voltammetry of P[Mn(III)Cl-TPP-2T] **P7a** and P[Co(II)-TPP-2T] **P4a** in CH₂Cl₂/TBAHFP (0.1 M), scan speeds 50, 75, 100, 125, 150 mV s⁻¹ from inwards to outwards.

which was electropolymerized on a interdigitated comb structure (distance between the two electrodes 10 μm) similar to that introduced by Wrighton *et al.*³⁴ The development of the relative conductivity of **P4a** at various potentials is shown in Fig. 7. An increase in conductivity is seen at potentials above 0.3 V whereas electroactivity starts at lower potentials (*ca.* 0.1 V). The maximum of conductivity is reached at 0.68 V which well coincides with the first oxidation peak of the porphyrin unit. At higher potentials the conductivity drops resulting in a bell-shaped curve and in the back scan a small hysteresis ($\Delta E = 25$ mV) develops. This is in accordance to studies by Zotti *et al.*^{3b,c} on ferrocene-functionalized polythiophenes for which a bell-shaped run of the conductivity curve is found indicating redox conductivity due to a hopping mechanism between redox centers. In contrast, charge transport only by polarons or bipolarons, *e.g.* in poly(3-methyl-2,2'-bithiophene), results in a

sharp sigmoidal shape of the curve with a broad plateau at the conductivity maximum of 20 mS. In comparison to this reference polymer, the relative maximum conductivity of the hybrid polymer **P4a** is diminished by a factor of 20.

Spectroelectrochemical properties of the polymer films

The optical properties of the novel porphyrin-functionalized polybithiophenes **P4a–P8a** in various oxidation states were investigated by spectroelectrochemistry. UV-Vis-NIR spectra of the polymer films electrochemically deposited on a platinum working electrode were recorded *in-situ* at various applied potentials in a reflection mode by means of a fiber optic.²¹ As reference, spectroelectrograms of separately synthesized subunits of the hybrid polymers, namely of poly(3-dodecyl-2,2'-bithiophene) and the metalated tetratolylporphyrins,

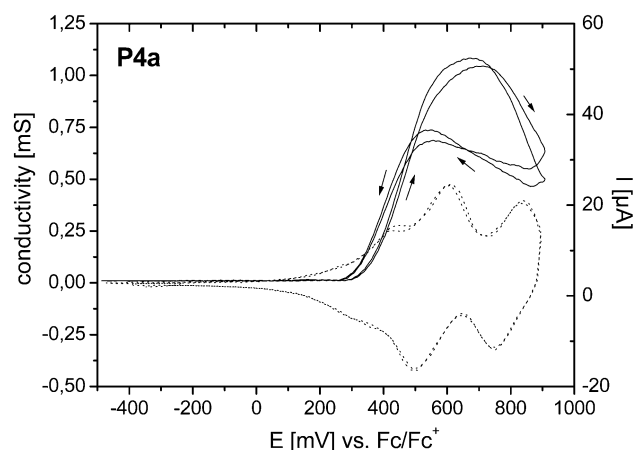


Fig. 7 *In-situ* conductivity (—) of a film of P[Co(II)TPP-2T] **P4a** in $\text{CH}_2\text{Cl}_2/\text{TBAHFP}$ (0.1 M) at a scan rate of 5 mV s^{-1} and $V_D = 10 \text{ mV}$ and a corresponding cyclic voltammogram (···) at a scan rate of 100 mV sec^{-1} .

respectively, were taken. In the neutral undoped state, the poly(alkylbithiophene) shows a typical $\pi-\pi^*$ transition band at $\lambda_{\text{max}} = 505 \text{ nm}$. Stepwise oxidation leads to a gradual decrease of the intensity in favour of the formation of rather broad polaron bands at $\lambda_{\text{max}} = 730 \text{ nm}$ and $\lambda_{\text{max}} = 1250-1600 \text{ nm}$. These merge together at higher potentials in a very broad bipolaron band with an absorption maximum around 1250 nm . On the other hand, the very intense Soret bands and the Q-bands of the metal porphyrins are shifted when either the oxidation state of the heteroaromatic core or of the central metal ion is changed.³⁵ In accordance with the electrochemical data, the spectroelectrograms of hybrid polybithiophenes **P4a–P8a** show an additive behaviour of the individual chromophores. Absorption maxima of their Soret-, Q- and $\pi-\pi^*$ bands are collected in Table 5. However, due to strong overlaps of the bands, the determination of peak maxima sometimes is rather difficult.

As a representative example, series of absorption spectra of P[Ni(II)-TPP-2T] **P5a** at various applied potentials vs. Ag/AgCl are shown in Fig. 8. When the potential is progressively increased from 0 V to 1.2 V, the $\pi-\pi^*$ band of the neutral conjugated backbone at $\lambda_{\text{max}} = 456 \text{ nm}$ decreases and simultaneously broad polaron and bipolaron bands become visible in the near-IR. The intense Soret ($\lambda_{\text{max}} = 403 \text{ nm}$) and Q-band ($\lambda_{\text{max}} = 532 \text{ nm}$) of the porphyrin subunit remain unchanged. Upon further oxidation (1.2 to 1.5 V), the latter bands decrease and a broad absorption ($\lambda = 575-800 \text{ nm}$) due to the formation of porphyrin radical cations evolve. Additionally, a new band at $\lambda_{\text{max}} = 337 \text{ nm}$ is visible which we attribute to the formation of a Ni(III) species. In contrast to the parent poly(alkylbithiophene), a further increase of the bipolaron band is not observed in this potential regime. We interpret this as being due to the fact that redox conductivity comes into play and charge transport in the polymer films now

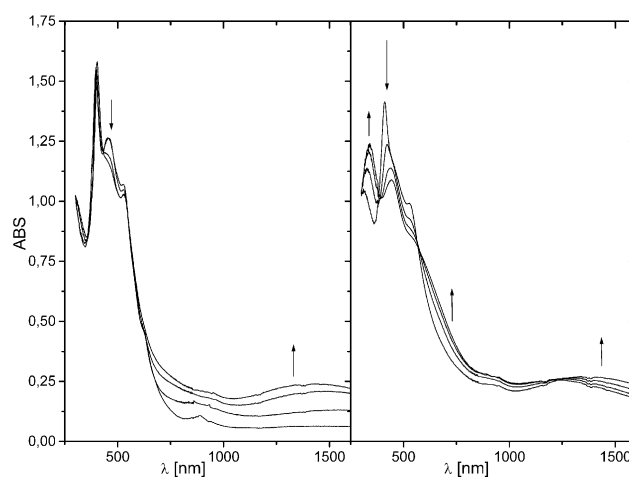


Fig. 8 Absorption spectra of P[Ni(II)-TPP-2T] **P5a** in $\text{CH}_3\text{CN}/\text{TBAHFP}$ (0.1 M) at 0–1.2 V vs. Ag/AgCl (left) and 1.2–1.5 V vs. Ag/AgCl (right).

partly occurs *via* hopping processes. As a consequence, positive charges are rather localized on the electronically decoupled porphyrin subunits than delocalized on the conjugated backbone. All these electrochemical processes are highly reversible, because on re-reduction to 0 V the original absorption spectrum of the film is recovered. Several isosbestic points in the absorption spectra additionally demonstrate the stability of the charged species and the lack of side reactions.

Application of porphyrin-functionalized polythiophenes as sensors

A great number of oxidation reactions, in particular in natural systems, are known to be catalyzed by metal porphyrin complexes and metal porphyrin containing enzymes, respectively.³⁶ The immobilization of (metallo)porphyrins in polymeric matrices or in monolayers on electrodes is therefore an attractive way to create redox-active modified surfaces for controlled electron transfer in catalytic epoxidations, hydroxylations or other oxidation reactions. Porphyrin-modified electrodes have therefore successfully been used in biosensors² or photovoltaic cells.⁶

We wanted to test the applicability of our novel hybrid polymer films in amperometric sensors. Since polychlorinated aromatics are hardly degradable herbicides and an iron porphyrin containing lignin peroxidase is able to dechlorinate these systems by oxidation to quinones,³⁷ we investigated the influence of 2,4,5-trichlorophenol on the electrochemical behaviour of P[Fe(III)Cl-TPP-2T] **P6a**. In Fig. 9 (left) a series of CVs is shown when the phenol is successively added to the electrolyte. Distinct shifts of the redox waves to more negative potentials are observed for the Fe(III)porphyrin, which are less pronounced for the polythiophene backbone, and depend on the phenol concentration. The modified electrode is sensitive in

Table 5 Absorption maxima of metalloporphyrin-functionalized polybithiophenes **P4a–P8a**

Compound	Soret		Q-bands			$\pi-\pi^*$ (PT) $\lambda_{\text{max}}/\text{nm}$
	$\lambda_{\text{max}}/\text{nm}$	$\lambda_{\text{max}}/\text{nm}$	$\lambda_{\text{max}}/\text{nm}$	$\lambda_{\text{max}}/\text{nm}$	$\lambda_{\text{max}}/\text{nm}$	
P[Co(II)-TPP-2T] P4a	412	531	—	—	—	^b
P[Co(III)-TPP-2T] P4a^a	437	522 (660) ^e	589	—	—	^b
P[Ni(II)-TPP-2T] P5a	403	532 ^f	—	—	—	456
P[Fe(III)Cl-TPP-2T] P6a	439 ^c	(630) ^{d,e}	—	—	—	^b
P[Zn(II)-TPP-2T] P8a	435 ^c	521 (690) ^e	563	596	652	^b

^a **P4a** after oxidation of Co^{2+} to Co^{3+} . ^b Superimposed by porphyrin Soret-band, maximum between 450 and 460 nm. ^c Superimposed by polybithiophene band. ^d Superimposed by polybithiophene band ^e Absorption maximum of porphyrin radical cation. ^f Superimposed by absorption maximum of porphyrin radical cation.

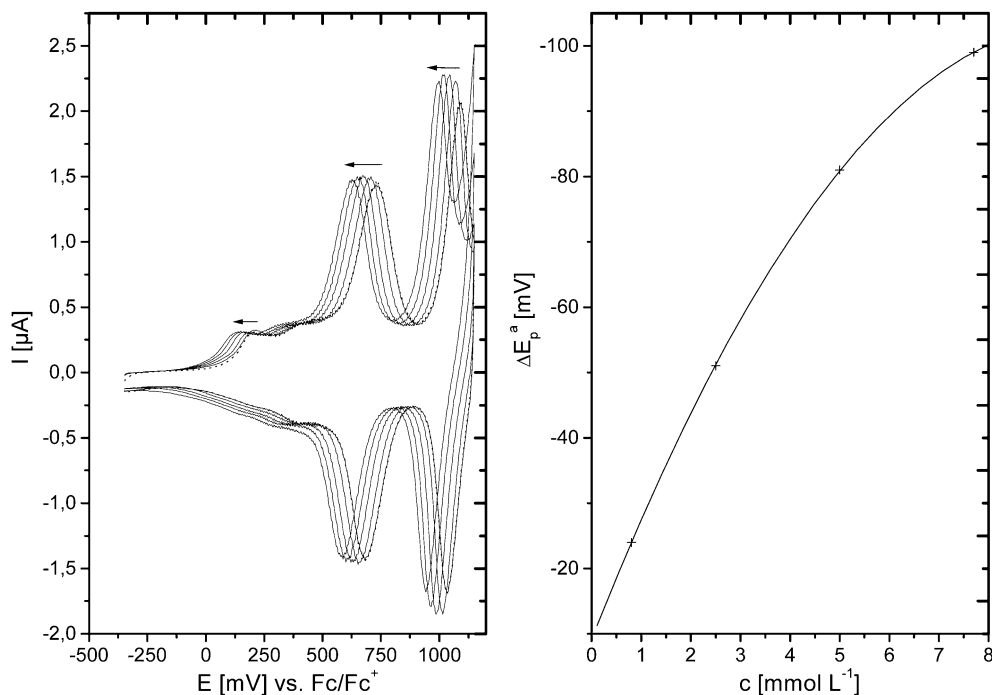


Fig. 9 Cyclic voltammograms of P[Fe(III)-TPP-2T] P6a in CH₂Cl₂/TBAHFP (0.1 M) under successive addition of 2,4,5-trichlorophenol ($c = 0, 8.0 \times 10^{-4}, 2.5 \times 10^{-3}, 5.0 \times 10^{-3}$ and 2.75×10^{-2} mol L⁻¹) (left). Calibration plot of the shift of the peak maxima of the first redox wave of the porphyrin subunit versus the concentration of the 2,4,5-trichlorophenol (right).

the sub-millimolar regime and ΔE increases to 100 mV for an 8×10^{-3} molar solution of phenol, and then saturation is observed (Fig. 9, right). Control experiments show that 2,4,5-trichlorophenol is electrochemically inactive within the applied potential regime, and that the electrochemistry of electrodes modified with the reference polymer, poly(3-alkyl-2,2'-thiophene) which does not contain porphyrin units, is not influenced by the phenol. These investigations demonstrate that the sharp redox wave of the porphyrin subunit represents a sensitive probe for external chemical stimuli promoting these hybrid polymers to potential candidates in amperometric sensors. The effects we observe are most probably due to interactions and complexation of the chlorinated phenols with the iron center which in turn alters the electronic properties of the porphyrin moiety and consequently its redox potentials. The transduction of this process into the change of the electrochemical response is only possible due to a mixed conduction mechanism in these hybrid materials.

Summary

We have described the synthesis as well as the electrochemical and optical properties of a series of novel (metallated) porphyrin-functionalized oligothiophenes **3–8**. The linkage of a *meso*-tetraphenylporphyrin moiety to a bi- or terthiophene unit via an alkyl spacer leads to monomers which after metallation of the porphyrin ligand can be electropolymerized to the corresponding metallo porphyrin-functionalized polythiophenes. Electrochemical and optical characterization of the polymer films reveals the superimposition of the electronic properties of the two π -systems. Spectroelectrochemical and conductivity measurements give information on the charge transport mechanism in these hybrid materials. Besides charge transport by polarons and bipolarons in the conjugated polythiophene matrix, electron hopping between isolated porphyrin redox centers plays a crucial role in the overall conduction mechanism. Formally, we created a hybrid of a conducting and a redox polymer leading to synergistic additional properties such as high redox stability, high charge loading capacity and sensitivity towards chemical stimuli.

Acknowledgements

The Fonds der Chemischen Industrie is gratefully acknowledged for financial support.

References

- 1 F. Garnier, *Angew. Chem.*, 1989, **101**, 529–533.
- 2 (a) S. Bernier, S. Garreau, M. Béra-Abérem, C. Gravel and M. Leclerc, *J. Am. Chem. Soc.*, 2002, **124**, 12463–12468; (b) G. Bidan, M. Billon, K. Galasso, T. Livache, G. Mathis, A. Roget, L. M. Torres-Rodriguez and E. Vieil, *Appl. Biochem. Biotechnol.*, 2000, **89**, 183–193; (c) H. Korri-Youssoufi, F. Garnier, P. Srivastava, P. Godillot and A. Yassar, *J. Am. Chem. Soc.*, 1997, **119**, 7388–7389; (d) M. Hiller, C. Kranz, J. Huber, P. Bäuerle and W. Schuhmann, *Adv. Mater.*, 1996, **7**, 219–222.
- 3 (a) O. Reynes, G. Royal, E. Chainet, J.-C. Moutet and E. Saint-Aman, *Electroanalysis*, 2003, **15**, 65–69; (b) G. Zotti, G. Schiavon, S. Zecchin, A. Berlin, G. Paganini and A. Canavesi, *Synth. Met.*, 1996, **76**, 255–258; (c) P. Bäuerle, M. Hiller, S. Scheib, M. Sokolowski and E. Umbach, *Adv. Mater.*, 1996, **8**, 214–218; (d) G. Zotti, S. Zecchin, G. Schiavon, A. Berlin, G. Paganini and A. Canavesi, *Chem. Mater.*, 1995, **7**, 2309–2315.
- 4 G. A. Sotzing, J. L. Reddinger, A. R. Katritzky, J. Soloduch, R. Musgrave, J. R. Reynolds and P. J. Steel, *Chem. Mater.*, 1997, **9**, 1578–1587.
- 5 (a) R. P. Kingsborough and T. M. Swager, *Chem. Mater.*, 2000, **12**, 872–874; (b) E. Steckhan, *Angew. Chem.*, 1986, **98**, 681–699.
- 6 J. Basu and K. K. Rohatgi-Mukherjee, *Sol. Energy. Mater.*, 1991, **21**, 317–325.
- 7 (a) S. Scheib and P. Bäuerle, *J. Mater. Chem.*, 1999, **9**, 2139–2150; (b) A. Emge and P. Bäuerle, *Synth. Met.*, 1999, **102**, 1370–1373; (c) P. Bäuerle and A. Emge, *Adv. Mater.*, 1998, **10**, 324–330; (d) K. B. Crawford, M. B. Goldfinger and T. M. Swager, *J. Am. Chem. Soc.*, 1998, **120**, 5187–5192; (e) T. Yamamoto, M. Omote, Y. Miyazaki, A. Kashiwazaki, B.-L. Lee, T. Kanbara, K. Osakada, T. Inoue and K. Kubota, *Macromolecules*, 1997, **30**, 7158–7165; (f) H. K. Youssoufi, M. Hmyene, A. Yassar and F. Garnier, *J. Electroanal. Chem.*, 1996, **406**, 187–194; (g) T. Benincori, E. Brenna, F. Sanniccolo, L. Trimarco, G. Moro, D. Pitea, T. Pilati, G. Zerbi and G. Zotti, *J. Chem. Soc., Chem. Commun.*, 1995, 881–882; (h) M. J. Marsella, P. J. Carroll and T. M. Swager, *J. Am. Chem. Soc.*, 1995, **117**, 9832–9841; (i) P. Bäuerle and S. Scheib, *Acta Polym.*, 1995, **46**, 124–129; (j) P. Bäuerle and S. Scheib, *Adv. Mater.*, 1993, **5**,

- 848–853; (k) P. N. Bartlett, A. C. Benniston, L.-Y. Chung, D. M. Dawson and P. Moore, *Electrochim. Acta*, 1991, **36**, 1377–1379.
- 8 (a) L. Cen, K. G. Neoh and E. T. Kang, *Biosens. Bioelectron.*, 2003, **18**, 363–374; (b) X. Liu, K. G. Neoh and E. T. Kang, *Langmuir*, 2002, **18**, 9041–9047; (c) P. Bäuerle and K.-U. Gaudl, *Adv. Mater.*, 1990, **2**, 185–188.
- 9 (a) A. Iraqi, J. A. Crayston and J. C. Walton, *J. Mater. Chem.*, 1998, **8**, 31–36; (b) P. Bäuerle, K.-U. Gaudl and G. Götz, *Springer Ser. Solid-State Sci.*, 1992, **107**, 384–389; (c) W. Schuhmann, R. Lammert, M. Haemmerle and H. L. Schmidt, *Biosens. Bioelectron.*, 1991, **6**, 689–697; (d) J. S. Foos, S. M. Degnan, D. G. Glennon and X. Beebe, *J. Electrochem Soc.*, 1990, **137**, 2530–2533.
- 10 (a) B. Jousselmé, P. Blanchard, E. Levillain, R. de Bettignes and J. Roncali, *Macromolecules*, 2003, **36**, 3020–3025; (b) P. A. van Hal, E. H. A. Beckers, S. C. J. Meskers, R. A. J. Janssen, B. Jousselmé, P. Blanchard and J. Roncali, *Chem. Eur. J.*, 2002, **8**, 5415–5429; (c) F. Effenberger and G. Grube, *Synthesis*, 1998, **9**, 1372–1379.
- 11 L. Huchet, S. Akoudad and J. Roncali, *Adv. Mater.*, 1998, **10**, 541–545.
- 12 (a) B. J. MacLean and P. G. Pickup, *J. Mater. Chem.*, 2001, **11**, 1357–1363; (b) J. Buey and T. M. Swager, *Angew. Chem.*, 2000, **112**, 623–625; (c) L. Trouillet, A. De Nicola and S. Guillerez, *Chem. Mater.*, 2000, **12**, 1611–1621; (d) P.-L. Vidal, B. Divisia-Blohorn, G. Bidan, J.-L. Hazemann, J.-M. Kern and J.-P. Sauvage, *Chem. Eur. J.*, 2000, **6**, 1663–1673; (e) J. L. Reddinger and J. R. Reynolds, *Chem. Mater.*, 1998, **10**, 1236–1243; (f) S. S. Zhu and T. M. Swager, *J. Am. Chem. Soc.*, 1997, **119**, 12568–12577; (g) S. S. Zhu, P. J. Carroll and T. M. Swager, *J. Am. Chem. Soc.*, 1996, **118**, 8713–8714; (h) T. Maruyama and T. Yamamoto, *Inorg. Chim. Acta*, 1995, **238**, 9–13; (i) M. O. Wolf and M. S. Wrighton, *Chem. Mater.*, 1994, **6**, 1526–1533; (j) T. Yamamoto, T. Maruyama, Z.-H. Zhou, T. Ito, T. Fukuda, Y. Yoneda, F. Begum, T. Ikeda, S. Sasaki, H. Takezoe, A. Fukuda and K. Kubota, *J. Am. Chem. Soc.*, 1994, **116**, 4832–4845; (k) N. Nishihara, T. Shimura, A. Ohkubo, N. Matsuda and K. Aramaki, *Adv. Mater.*, 1993, **5**, 752–754.
- 13 (a) S. Cosnier, C. Gondran, R. Wessel, F.-P. Montfors and M. Wedel, *J. Electroanal. Chem.*, 2000, **488**, 83–91; (b) B. A. Bettelheim, S. A. White, R. W. Raybuck and R. W. Murray, *Inorg. Chem.*, 1987, **26**, 1009–1017; (c) A. Deronzier and J.-M. Latour, *J. Electroanal. Chem.*, 1987, **224**, 295–301.
- 14 F. Bedioui, J. Devynck and C. Bied-Charreton, *Acc. Chem. Res.*, 1995, **28**, 30–36.
- 15 F. Bedioui, P. Moisy, J. Devynck, L. Salmon and C. Bied-Charreton, *J. Mol. Catal.*, 1989, **56**, 267–275.
- 16 (a) R. Iqbal, G. Yahioğlu, L. Milgrom, S. C. Moratti, A. B. Holmes, F. Cacialli, J. Morgado and R. H. Friend, *Synth. Met.*, 1999, **102**, 1024–1025; (b) B. Jiang and W. E. Jones, *Macromolecules*, 1997, **30**, 5575–5581; (c) Z. Bao, Y. Chen and L. Yu, *Macromolecules*, 1994, **27**, 4629–4631.
- 17 (a) F. Bedioui, C. Bongars, J. Devynck, C. Bied-Charreton and C. Hinnen, *J. Electroanal. Chem.*, 1986, **197**, 87–99; (b) O. Ikeda, K. Okabayashi, N. Oshida and H. Tamura, *J. Electroanal. Chem.*, 1985, **191**, 157–174; (c) K. Okabayashi, O. Ikeda and H. Tamura, *J. Chem. Soc., Chem. Commun.*, 1983, 684–685.
- 18 (a) T. Malinski, A. Ciszewski, J. R. Fish, E. Kubaszewski and L. Czuchajowski, *Adv. Mater.*, 1992, **4**, 354–357; (b) J. R. Fish, E. Kubaszewski, A. Peat, T. Malinski, J. Kaczor, P. Kus and L. Czuchajowski, *Chem. Mater.*, 1992, **4**, 795–803.
- 19 (a) M. R. Tschudi, S. Mesaros, T. F. Lüscher and T. Malinski, *Hypertension*, 1996, **27**, 32–35; (b) S. Trevin, F. Bedioui and J. Devynck, *Talanta*, 1996, **43**, 303–311; (c) T. Malinski and Z. Taha, *Nature*, 1992, **358**, 676–678.
- 20 M. Schäferling and P. Bäuerle, *Synth. Met.*, 1999, **101**, 38–39.
- 21 J. Salbeck, *J. Electroanal. Chem.*, 1992, **340**, 169–195.
- 22 The interdigital arrays were provided by Fraunhoferinstitut für physikalische Messtechnik in Freiburg, Germany.
- 23 (a) G. Etemad-Moghadam, C. Ding, F. Tadj and B. Meunier, *Tetrahedron*, 1989, **45**, 2641–2648; (b) R. G. Little, J. A. Anton, P. A. Loach and J. A. Ibers, *J. Heterocycl. Chem.*, 1975, **12**, 343–349.
- 24 (a) P. Bäuerle, F. Würthner, G. Götz and F. Effenberger, *Synthesis*, 1993, 1099–1103; (b) P. Bäuerle, F. Würthner and S. Heid, *Angew. Chem.*, 1990, **102**, 414–415; P. Bäuerle, F. Würthner and S. Heid, *Angew. Chem., Int. Ed. Engl.*, 1990, **29**, 419–420.
- 25 A. D. Adler, F. R. Longo, F. Kampas and J. Kim, *J. Inorg. Nucl. Chem.*, 1970, **32**, 2443–2445.
- 26 R. D. Jones, D. A. Summerville and F. Basolo, *J. Am. Chem. Soc.*, 1978, **100**, 4416–4423.
- 27 (a) R. J. Abraham, I. Marsden and L. Xiuqing, *Magn. Reson. Chem.*, 1990, **28**, 1051–1057; (b) H. M. Goff and A. P. Hansen, *Inorg. Chem.*, 1984, **23**, 321–326; (c) R. C. Parmely and H. M. Goff, *J. Inorg. Biochem.*, 1980, **12**, 269–280; (d) G. N. La Mar and F. A. Walker, *J. Am. Chem. Soc.*, 1975, **97**, 5103–5107; (e) R. J. Abraham, G. E. Hawkes, M. F. Hudson and K. M. Smith, *J. Chem. Soc., Perkin Trans. 2*, 1974, 204–211; (f) R. J. Abraham, G. E. Hawkes and K. M. Smith, *J. Chem. Soc., Perkin Trans. 2*, 1974, 627–634; (g) G. N. La Mar and F. A. Walker, *J. Am. Chem. Soc.*, 1973, **95**, 1790–1795; (h) G. N. La Mar, G. R. Eaton, R. H. Holm and F. A. Walker, *J. Am. Chem. Soc.*, 1973, **95**, 63–75.
- 28 L. R. Milgrom, *The Colours of Life*, Oxford University Press, Oxford, UK, 1997.
- 29 (a) L. Edwards, D. Dolphin, M. Gouterman and A. D. Adler, *J. Mol. Spectr.*, 1971, **38**, 16–32; (b) L. J. Boucher, *J. Am. Chem. Soc.*, 1968, **90**, 6640–6645; (c) D. W. Thomas and A. E. Martell, *J. Am. Chem. Soc.*, 1956, **78**, 1335–1343; (d) G. D. Dorough, J. R. Miller and F. M. Huennekens, *J. Am. Chem. Soc.*, 1951, **73**, 4315–4320.
- 30 K. M. Kadish, *Chem. Rev.*, 1985, 435–605.
- 31 J.-H. Fuhrhop, K. M. Kadish and D. G. Davis, *J. Am. Chem. Soc.*, 1973, **95**, 5140–5147.
- 32 (a) B. Ballarin, R. Seeber, L. Tassi and D. Tonelli, *Synth. Met.*, 2000, **114**, 279–285; (b) B. Ballarin, S. Masicro, R. Seeber and D. Tonelli, *J. Electroanal. Chem.*, 1998, **449**, 173–180.
- 33 (a) B. Krische and M. Zagorska, *Synth. Met.*, 1989, **28**, 257–268; (b) P. Marquie, J. Roncali and F. Garnier, *J. Electroanal. Chem.*, 1987, **218**, 107–118.
- 34 (a) H. S. White, G. P. Kittleson and M. S. Wrighton, *J. Am. Chem. Soc.*, 1984, **106**, 5375–5377; (b) G.-P. Kittleson, H. S. White and M. S. Wrighton, *J. Am. Chem. Soc.*, 1984, **106**, 7289–7296.
- 35 (a) F. D'Souza, A. Villard, E. Van Caemelbecke, M. Franzen, T. Boschi, P. Tagliatesta and K. M. Kadish, *Inorg. Chem.*, 1993, **32**, 4042–4048; (b) A. Wolberg and J. Manassen, *J. Am. Chem. Soc.*, 1970, **92**, 2982–2991.
- 36 B. Meunier, *Chem. Rev.*, 1992, **92**, 1411–1456.
- 37 B. Meunier and A. Sorokin, *Acc. Chem. Res.*, 1997, **30**, 470–476.